(PREPRINT) AAS 11-XXX

ONBOARD ATMOSPHERIC MODELING AND PREDICTION FOR AUTONOMOUS AEROBRAKING MISSIONS

Robert H. Tolson and Jill L. H. Prince

Aerobraking has proven to be an effective means of increasing the science payload for planetary orbiting missions and/or for enabling the use of less expensive launch vehicles. Though aerobraking has numerous benefits, large operations cost have been required to maintain the aerobraking time line without violating aerodynamic heating or other constraints. Two operations functions have been performed on an orbit by orbit basis to estimate atmospheric properties relevant to aerobraking. The Navigation team typically solves for an atmospheric density scale factor using DSN tracking data and the atmospheric modeling team uses telemetric accelerometer data to recover atmospheric density profiles. After some effort, decisions are made about the need for orbit trim maneuvers to adjust periapsis altitude to stay within the aerobraking corridor. Autonomous aerobraking would reduce the need for many ground based tasks. To be successful, atmospheric modeling must be performed on the vehicle in near real time. This paper discusses the issues associated with estimating the planetary atmosphere onboard and evaluates a number of the options for Mars, Venus and Titan aerobraking missions.

INTRODUCTION

The first planetary aerobraking (AB) mission, Venus Magellan, took 70 days and over 700 passes[1] through the atmosphere for the purpose of enhancing the scientific return of the extended mission. Aerobraking was performed to reduce the orbital eccentricity after the primary science mission thereby lowering apoapsis altitude and improving the resolution of the gravity mapping. Based on the successful Magellan experience, AB became an enabling technology for recent Mars orbiting missions. These missions had AB operational phases that took about 850 orbits for Mars Global Surveyor (MGS), 77 days and 325 orbits for Mars Odyssey (ODY), and 145 days and 420 orbits for Mars Reconnaissance Orbiter (MRO). MGS was anomalistically long due to a broken solar array which constrained the maximum dynamic pressure during an AB pass. These missions used the solar arrays as the primary drag area and consequently, except for MGS, the temperature of the solar arrays was the limiting atmosphere dependent factor in designing the AB corridor,[1] although other subsystems had to also be considered.

Although AB has numerous benefits, there are also cost and risk. The greatest costs are the large operations team and DSN coverage that have been required to maintain the AB schedule. The greatest risk[2] has been the inability to predict the orbit to orbit variability of the Martian atmosphere. One of the functions performed on an orbit by orbit basis is an estimation of the atmospheric density profile. These profiles were recovered using telemetric accelerometer and gyro data (IMU). After the AB pass, these data were related to aerodynamic forces and then mapped into atmospheric density at one second intervals along the orbit. The recovered density profiles were analyzed to determine atmospheric temperature, gravity wave phenomena, orbit to orbit variability, longitude dependent wave characteristics, latitudinal gradients and other information.[3] To predict upcoming atmospheric conditions, this information was evaluated on a day-by-day basis by a team of atmospheric scientist, the Atmospheric Advisory Group (AAG). Imple-

mentation of autonomous AB will require the development of robust, reliable, and simple methods for the estimation of atmospheric density profiles from the IMU data and the prediction of future atmospheric conditions without the human interpretation provided by the AAG.

Mars, Venus and Titan are targets for autonomous AB missions. It is well know that the Mars atmosphere provides a challenging environment for autonomous AB because of the high orbit to orbit variability in atmospheric density.[3] An abundance of AB data provides adequate information for testing autonomous AB at Mars. High orbit to orbit variability has also been detected near the terminator and on the night side of Venus,[4] but there are no accelerometer data for validation or detection of small scale variations. Little is known about the variability of the Titan atmosphere on the temporal and spatial scales of interest for AB. However, during the Huygens descent through the atmosphere, significant wave structure was found in the density and temperature profiles in the altitude range of interest,[5] and Cassini mass spectrometer measurements during Titan flybys in the altitude range from 1000 to 1600 km identified relevant vertical and horizontal wave structure in various constituents and in total density.[6]

The current paper presents various potential methods for representing density profiles derived from IMU data during AB, for recovering profile parameters from IMU data, and for optimal combinations of profiles for prediction. Algorithms are evaluated based on simplicity, robustness, and applicability to onboard limitations. The atmospheres of Mars is the primary focus due to the wealth of data, but Venus and Titan are discussed biriefly.

ATMOSPHERIC ESTIMATION DURING PAST AEROBRAKING MISSIONS

Magellan entered orbit in August 1990 with an orbit eccentricity of about 0.4. After the 4-th Venusian day, spanning over 7000 orbits, the AB phase was initiated to reduce the eccentricity to about 0.03 after 70 days and over 700 AB passes. During AB, the active side of the solar array was turned away from the free stream direction to minimize the temperature encountered by the cells, adhesives and structure. Maximum solar array (SA) temperature was the limiting factor constraining the rate of AB.[1] Pre-aerobraking studies provided a relationship between free stream dynamic pressure and maximum SA temperature, but atmospheric density was required to determine dynamic pressure. The method for determining atmospheric density during each Magellan pass relied on Doppler radio tracking data. Pre-pass and post-pass tracking data were process in a single orbit determination (OD) that included density at a specified altitude as a solution parameter. This approach provides continuity of the equations of motion across the unobserved AB pass. To provide a unique solution for density, a model for density vs. altitude was used. The contemporary VIRA model[7] provided density every 5 km and a constant scale height was used for interpolation. Density at 140 km altitude was the solution parameter in the OD process and the scale heights from the VIRA model were used to map density to other altitudes. For a hydrostatic atmosphere, this is equivalent to assuming that the temperature profile is given and the density profile is defined within a multiplicative factor.

Magellan AB was so successful that AB was considered a validated technology and was enabling for the MGS mission in 1997. The MGS AB corridor was again defined in terms of the surrogate variable, free stream dynamic pressure. However, after the discovery of the broken solar array on orbits 11 through 15, the corridor criteria changed from limiting SA temperature to limiting torque on the broken SA yoke[8] and for the only time, the maximum dynamic pressure became the most relevant control variable.

During MGS operations, density at periapsis was estimated by two different methods. Members of the AAG used the IMU data at a one per second sample rate to model the atmospheric density profile. IMU accelerometer measurements were mapped to the vehicle center of mass using the IMU angular rate data and the resulting center of mass acceleration was converted to atmospheric density using a data base of aerodynamic force coefficients. Density at periapsis and density scale height were extracted using a least squares solution from three data sets that included all data within 1, 1.5 and 2 scale heights of periapsis.[9] The "best" model was selected by visual comparison of the model and the data density profiles. Estimated scale heights were averaged over a few orbits and provided to the NAV team to be used for corridor control maneuver calculations and orbit determination. The NAV team used this scale height to estimate the density at periapsis using radio tracking data in the same way as was done for Magellan. The need for more autonomy[10] was recognized well before the end of the 15 months required to complete MGS AB. When adjusted for the different between predicted and observed scale height (equation (A-5)), the AAG and NAV estimates of periapsis density were within 3%, 1σ.

The periapsis altitude, latitude, density at periapsis, local solar time, density scale height, and solar longitude as determined during operations, are shown in Figure 1. In an idealized atmosphere, density scale height is proportional to temperature, so this variable can be thought of as the local average atmospheric temperature. The first 202 orbits of MGS were termed "phase 1," after which there was a six month "hiatus" while periapsis precessed over the north pole at a periapsis altitude near 170 km. Aerobraking "phase 2" began on orbit 573 and ended on orbit 1285 about 2 weeks after periapsis precessed over the south pole during the winter.

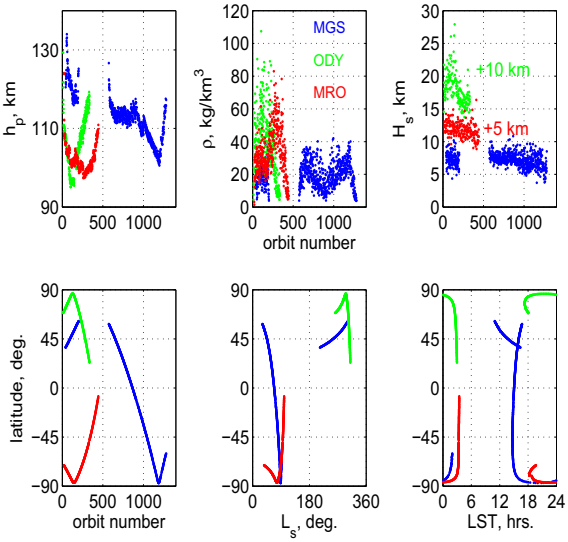

Figure 1. Summary of aerobraking conditions for MGS, ODY and MRO.

ODY, the most aggressive AB mission, went to the lowest altitude and experienced the highest densities, unintentionally reaching 107 kg/km^3 on orbit 106. Like MGS and MRO, the science orbit required a particular LST, which meant that the AB phase had to end within a few days of the planned final day. Both ODY and MRO used MarsGRAM[11] to define the density profile and the OD process determined the density by solving for a multiplier to be applied to the MarsGRAM density profile. In addition, as the latitude of AB precessed toward the north pole, it was expected that thermospheric temperature would decrease. Instead the temperature increased dramatically as indicated by the density scale height in Figure 1. The inferred temperature increase has been interpreted as a polar warming[12] and lead to accelerometer derive density scale heights between 7 and 14 km with an average above 10 km. The nominal atmosphere scale height was expected to be closer to 6 km and did returned to that value after the latitude was south of 60°N. The difference in scale height partially lead to the large density differences between MarsGRAM and the IMU derived densities.

ODY also tested a couple of new techniques. Though ODY used maximum dynamic pressure to define the AB corridor, it was the first mission to have a near real time prediction of the solar array temperatures for a comparison with the measured temperatures.[13] Based on this comparison

over a number of orbits, the AB safety margin was reduced, permitting ODY AB to proceed at a faster rate. During this mission the first onboard algorithm,[14] called the Periapsis Timing Estimator (PET), designed to reduce the work load of the ground flight team, was tested.

MRO had a less risky AB phase than ODY because there was 6 months between MOI and the time when the orbit would have the proper local solar time (LST). Aerobraking was initially performed with nearly a 200% safety margin as opposed to the 100% margins used for MGS and ODY. However, as suggested by the significant increase in density after orbit 200, MRO fell behind the time line during the early conservative approach and AB was more aggressive for the last 200 orbits. PTE was used operationally during this mission with an estimated saving of about $1m dollars. The operational process was essentially the same as Odyssey.

ATMOSPHERIC PREDICTION PERFORMANCE DURING OPERATIONS

During Mars AB operations, the AAG monitored the characteristics of recent AB passes to anticipate major changes in the atmosphere. The simplest variation used for modeling the density (ρ) profile was the exponential or constant scale height (CSH) model

$$\rho(h) = \rho_p \exp\left[\frac{-(h-h_p)}{H_s}\right] \tag{1}$$

where density, as determined from IMU data,[9] is a function only of the altitude (h) above some reference or base altitude, here taken as periapsis, with the density at h_p of ρ_p and density scale height (H_s). Such a model results for a homogeneous, isothermal atmosphere in hydrostatic equilibrium, and the density scale height is related to the atmospheric temperature (T), the local gravity acceleration (g) and the mean molecular weight by $H_s = kT/mg$, where k is the Boltzmann constant. Using this as the basic model, the group studied density and temperature latitudinal gradients, amplitude of gravity waves, and among others, the accuracy of predicting the periapsis density for the next orbits using the density and scale height from the current orbit. This latter metric was called "persistence' and is a measure of the atmospheric variability that the AB system must accommodate. The ratio of observed to predicted periapsis density for orbit n+1 is

$$\frac{\rho_{obs_{n+1}}}{\rho_{pred_{n+1}}} = \frac{\rho_{obs_{n+1}}}{\rho_{obs_n}} \exp\left[\frac{h_{n+1}-h_n}{H_{s_n}}\right] \tag{2}$$

where the altitudes are provided by the OD process and "observed" density and scale height are determined from IMU data. Orbit n is called the "base' orbit and orbit n+1 is the "predict" orbit.

Figure 2 provides the persistence for all three Mars missions. The means over the entire missions are between 1.06 and 1.08, with the deviation from unity mostly being an artifact of averaging a positive ratio. ODY has the largest 19 orbiting running mean at 1.38 and maximum standard deviation of 1.10, i.e. over a factor of two variation orbit to orbit. Mission wide standard deviations range form 37% for MRO to 47% for ODY. The large ODY value perhaps due to the very large variations early in the mission between 70^o and 80^o latitude. Except for ODY during this time, the deviations from the means are much smaller at high latitudes than in the mid latitudes and equatorial regions. Poleward of 60^o latitude, the 1σ deviations are generally between 20% and 30%. Just from a geometric argument, it might be expected that the deviations would become smaller near the pole since great circle distances between successive periapsis locations become shorter. The large ODY deviations near the pole are likely due to the polar warming producing strong winds and large, asymmetric temperature variations around the pole.[12,15] In the tropics

persistence is the largest for all three missions likely due to the global scale tides that appear as stationary waves.[16] These waves were sufficiently persistent and observable during MGS that models were developed during operations to include their influence on predicting subsequent periapsis densities and to plan orbit trim maneuvers. Latitude dependent empirical models were developed post flight for inclusion of such waves in Monte Carlo simulations of AB missions.[17] These waves appeared for brief periods during ODY and MRO, but not with sufficient persistence to be included in operational decisions.

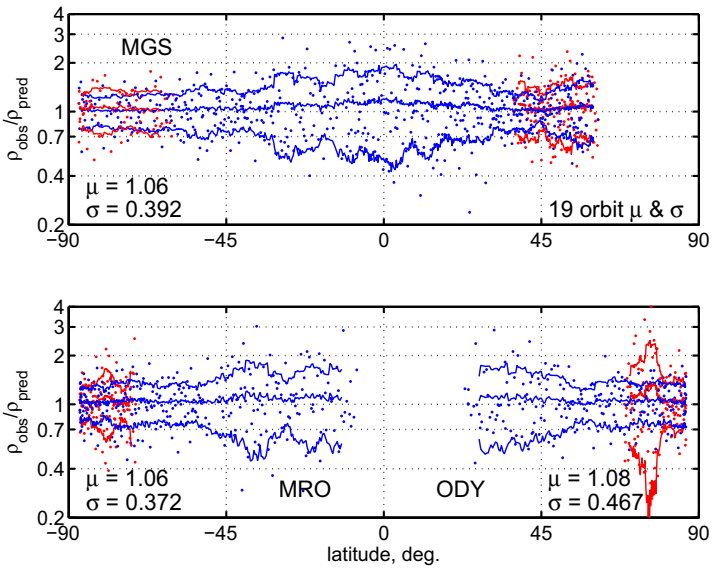

Figure 2. Persistence for MGD, ODY and MRO missions. Dots are data and lines are the 19 orbit running mean and mean +/- one standard deviation. Total mission μ and σ are also shown. Dots and lines change color as periapsis regresses past the pole.

Ignoring the latitudinal, seasonal, diurnal and other dependencies and considering the orbit to orbit variability as a random process provides very similar results for all three missions. It was found[17] that persistence can be reasonably represented by a gamma probability distribution. Maximum likelihood estimates (95%) of the two gamma distribution parameters for each mission results in probability density distributions shown in Figure 3. The histograms are from the same ratios shown in Figure 2. Within the 95% confidence interval, the values of σ and μ are indistinquishable from each other and compare well with the simple standard deviations in Figure 2. Since underestimating density is usually of higher mission risk than underestimation, these distributions can be used to approximate the probability associated with any ratio of ρ_{obs} to ρ_{pred}. For example, for MGS, ODY and MRO, the probabilities that the ratio will be less than 2 are 98.5%, 97% and 98.6% respectively. These probabilities are consistent with the AB rule of thumb requiring a design safety factor of 2 uncertainty in density. The distributions might also be used for Monte Carlo simulations of AB missions.

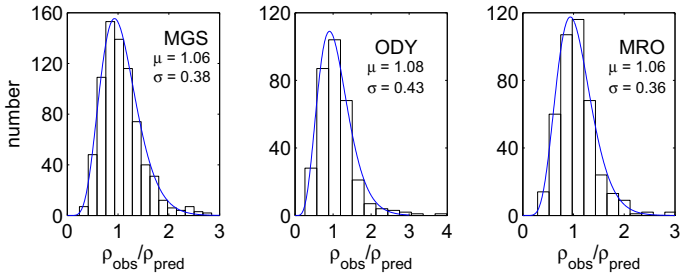

Figure 3. Gamma probability density distribution based on maximum likelihood fits to persistence data for three Mars aerobraking missions.

RELEVANT ATMOSPHERIC PARAMETERS FOR AEROBRAKING

The relevant atmospheric parameters depend on the criterion selected to define the AB corridor. If the limiting condition is related to maximum aerodynamic force or torque, then maximum dynamic pressure is likely the relevant parameter. If maximum temperature is the limiting factor for a component with rapid thermal response, maximum free stream heat flux might be the relevant parameter. If temperature is the limiting factor for a component with slow thermal response

(e.g. high thermal inertia or low radiative cooling), total or integrated heat flux may be most relevant. Here thermal response time is relative to the duration of the AB pass. To calculate any of these parameters requires knowledge of some characteristic of atmospheric density along the trajectory. To predict the variation for subsequent orbits requires an atmospheric model.

For this discussion, consider Figure 4 which shows the recovered density vs. time and vs. areodetic altitude for a typical Mars AB orbit. A least squares fit to data with $\rho>2$ kg/km^3 using the CSH model produced the "model" results. For this orbit, maximum density occurs 57 sec. before periapsis, a feature not captured by CSH. There is considerable asymmetry in the time profile, with density rising faster than it falls. If maximum dynamic pressure or maximum heat flux are the selected corridor criteria, then recovering the density at periapsis using the data or the model is inadequate. Further, when maximum temperature is the criterion, the shape of the heat flux as well as the total heat flux could become a consideration and only a detailed thermal analysis[18] can address these issues. The CSH scale height of 8.9 km, which might be used to predict density for the next orbit, represents the inbound, outbound and mean density profiles reasonably well. Maximum density occurs 2 km above periapsis and density varies by nearly a factor of 3 within this altitude range. This gradient is likely due to a strong along track density gradient. Within this range, ODY spend about 110 seconds and traveled about 360 km along track. The high frequency deviation from a "smoothed" density profile are generally attributed to gravity waves[19] and are a common feature at high latitudes. Note that accelerometer noise becomes relevant above altitudes of 125 km. Early and late in the AB pass, accelerometer data noise dominates the signal and the recovered "density" is often negative. These phases of the pass are used to determine a time linear approximation to the accelerometer bias, which is used to correct the data during the pass.[9]

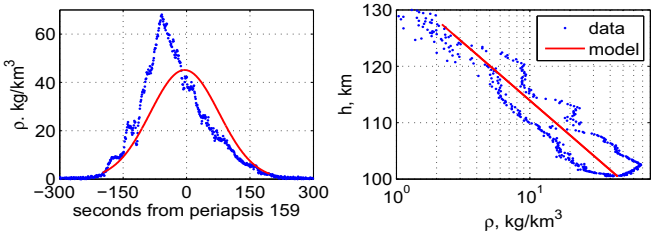

Figure 4. ODY orbit 159 atmospheric density inferred from accelerometer data

Although the density variation is usually modeled as a function of only altitude, as seen above, along track variations may dominate over the altitudinal. Large scale variations in atmospheric properties, from those assumed for the simple CSH model, might be expected to include an along track variation in base density and/or base temperature, and an altitudinal variation in temperature. Examples of how such variations affect the density profiles are shown in Figure 5.

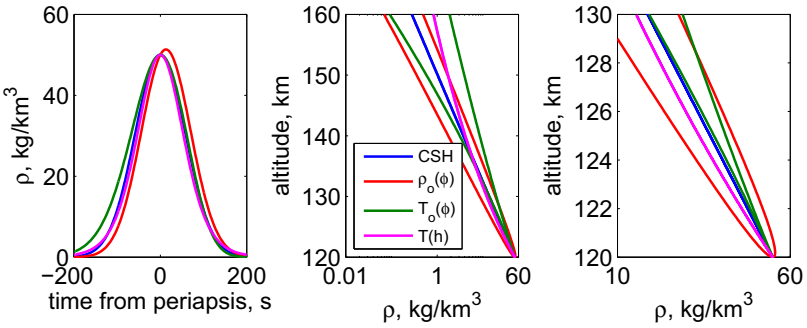

Figure 5. Effects of along track and altitudinal density and temperature gradients on density profiles.

Although there are obvious deviation in the altitudinal profiles, the differences in the temporal variation are more subtle. The CSH model is of course a straight line in the two right panels and for this case has a scale height of 7 km. Assuming base density varies linearly with along track angle (ϕ) provides different inbound and outbound profiles and a substantial difference in the two

densities within a kilometer or two of periapsis that is comparable with the altitudinal variation in density. An along track linear temperature variation produces a linear variation in scale height resulting again in different inbound and outbound profiles. This variation causes little density differences in the vicinity of periapsis but an increasing difference with altitude. The model with temperature increasing linearly with altitude (T(h)) has the same inbound and outbound altitude profiles and no significant deviation in the first 10 km, but deviates significantly altitudes 20 km above periapsis and higher. One can assume that some combination of these and other effects influence every AB pass. For autonomous AB the first issue is to quantify such effects and the second issue is to decide whether or not to include them in the atmospheric estimation process.

As examples of some of the multiplicity of effects on real AB passes, consider Figure 6 which provides examples of Odyssey profiles that are representative of the types of phenomena seen during all the Mars AB missions. The noticeable increase in data noise level is due to halving the sample rate on orbit 134 and again on orbit 270. Clearly the "bell shaped" density variation with time, derived in APPENDIX I, is not representative of any of these orbits. For orbit 44, the factor of two change in density over 10 seconds is not atypical for Mars. The time or altitude of maximum density are meaningless concepts for pass 157. The large asymmetry for orbit 159 results in maximum density occurring a full minute before periapsis. Generally solar power and Earth communications are lost during the AB pass. Thus there are clear reasons to want to minimize the duration that the vehicle is in the AB orientation. The AB phase is usually designed to be centered on periapsis. With such large asymmetries, extra time may have to be allocated, or if the asymmetries are consistent from orbit to orbit, biasing the center of the pass away from periapsis may be desirable. The AB passes for orbits 157 and 159 are 7 hours apart in time, 2 km apart in altitude and essentially at the same latitude, yet the profiles and the maximum density are dramatically different. These phenomena are the sort of natural orbit to orbit variability that are difficult to predict and therefore must be included as uncertainties in the design of any AB mission and requires a particularly robust design for an autonomous AB mission. It will be seen that there is some orbit to orbit persistence in the density, density scale height and temporal asymmetry.

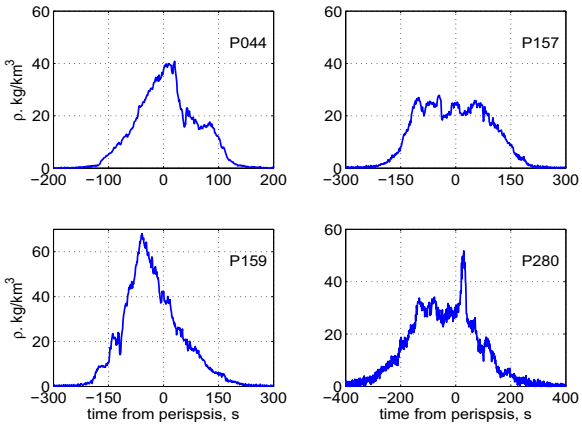

Figure 6. Four Odyssey orbits.

Near factor of two density spikes like P280 are uncommon but would be important if maximum density or heat flux is the consideration and not so important if total heat flux is the consideration. Even in the former case, the characteristic response time of the system will play a role. At Mars, the lack of persistence in the shape and maximum value of the density profile from orbit to orbit and the small-scale deviation are attributed to global scale longitudinal waves and vertically propagating gravity waves. The longitudinal waves during MGS have been modeled[17] and are attributed to non-migrating thermal tides[16] in the lower atmosphere that propagate to the upper atmosphere in the equatorial and mid-latitude regions. On the other hand, the source of the gravity waves is not known, but they are believed to originate in the lower atmosphere and, at high latitudes, propagate vertically while increasing in amplitude with subsequent "breaking" in the lower thermosphere.[19] Their latitudinal, seasonal, diurnal variations of rms amplitude have been par-

tially defined from previous AB data.[3] Whether or not they are significant for a particular mission depends on the criteria that limit AB. In the modeling approaches that follow, neither of these wave types will be a consideration as they are very difficult to model at this time.

The observed density asymmetries in time could be due to either an along track density gradient at a fixed altitude or to the areodetic altitude gradient at a constant distance from the center of the planet. First consider a possible density gradient. ODY, like the other Mars AB missions, is in a near polar orbit so along track is essentially latitudinal. The polar regions are generally colder than the tropics and consequently density scale height is smaller in polar regions. This would suggest that, for a fixed altitude, a lower density would be expected near the pole than in the tropics and strong latitudinal density gradients have been seen in all three Mars missions. On the second possible reason for a density asymmetry, periapse is the point in the orbit that is closest to the center of mass; but, due to planetary flattening, does not usually correspond to the point of lowest areodetic altitude. Planetary flattening is defined by the reference ellipsoid which approximates the equipotential surface at the surface of the planet. The reference ellipsoid is selected to approximate such a surface by defining an equatorial radius (a) and a flattening (f) that give a polar radius of a(1-f). For the Earth, the ellipsoid can be thought of as defining "mean sea level." On solid planets, the ellipsoid is selected to provide an equatorial radius that approximates the physical mean radius and the flattening is usually selected to represent the equipotential defined by the central gravitational potential, J_2 and the centrifugal potential due to planetary rotation. In an idealized, isothermal atmosphere, surfaces of constant planetodetic altitude correspond to surfaces of constant pressure and density. Hence, in a real atmosphere, density should be approximately constant on surfaces of constant planetodetic altitude. Many empirical atmospheric models, as will this paper, use this surface as the reference from which altitude is measured.

Density: In this paper it is assumed that the AB corridor is defined in terms of variables that require a knowledge of atmosphere density along the trajectory. But it should be kept in mind that density is almost always a surrogate for some other physical quantity that actually defines the limits on the execution of AB.

Density Scale Height: Density scale height plays two roles in AB. First, for maneuver calculations to stay within a density related corridor, the density scale height must be known to calculate the required dV. Second, if total heat flux or integrated density is important, the integral depends on the reference altitude density and the scale height as shown by equation (A-5).

Asymmetry of Density Profile: As mentioned above, during AB at Venus or Mars, the vehicle would be generally turned from sun-point and would be operating on batteries. In this case it may be desirable to minimize the time in the AB orientation. If the density profile is skewed or asymmetric in time, an allowance may be made for the potential skewness. If the skewness is predictable, then it can be included in the design and the AB pass can be accordingly biased in time.

Figure 7 shows the influence of planet flattening on shifting the density profile for a Mars AB mission. The upper left chart provides the variation of altitude above periapsis along the orbit, where the orbit parameters are given in the figure. The second line shows the variation in altitude above the reference ellipsoid along the orbit. The upper right panel provides the difference over three density scale heights or 21 km. The lowest areodetic altitude and highest density occurs 64 seconds before periapsis. The 0.59 km difference in altitude would cause a 9% higher density than the density at periapsis. This shift would also cause a least squares density estimation process, centered on periapsis, to overweight the outbound leg of the pass.

The time and altitude shifts for other latitudes and orbit periods are shown in the lower two panels. The difference of course approach zero at the equator and pole, are maximum at mid latitudes, and decrease rapidly at the orbit period increases. This latter effect is due to the shortening of the duration (equation (A-6))of the pass as orbit eccentricity increases for a fixed periapsis altitude and an increasing orbital period. Non-polar orbits will of course show smaller effects at every latitude. The size of the altitude difference and time shift are increased with planetary flattening, AB pass duration and angular velocity at periapsis. This phenomena is not an issue at Venus due to very slow rotation and the nearly spherical gravity field. The Titan rotational period is 15.9 days and Saturn produces tidal bulges of less than one kilometer resulting in a flattening that is less than 1/10 of Mars, so the effects of Titan AB are likely ignorable.

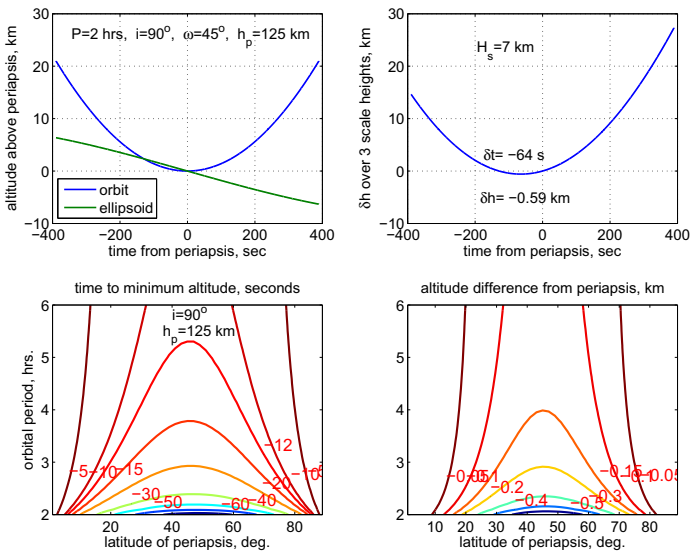

Figure 7. Mars reference ellipsoid flattening effect on density profiles.

POTENTIAL ATMOSPHERIC MODELS AND USES

Here it is assumed that no preflight empirical model of the atmosphere exist that is accurate enough to perform AB without using onboard data to adjust model parameters during the flight. Selection criteria for onboard atmospheric models include (1) capture the relevant characteristics of the atmosphere, (2) be robust against unexpected phenomena, (3) allow for linear estimation of the parameters, (4) permit prediction of atmospheric properties for the next AB pass and (5) support the calculation of corridor control maneuvers. A number of models are discussed and evaluated using Mars AB data. All the models assume that atmospheric density data have been derived from an onboard source, e.g IMU accelerometer and gyro data.

Constant Scale Height

The constant scale height model (CSH) given by equation (1) was used successfully as the fundamental model during the MGS mission. There are two disadvantages to using this form for estimation. First, the density is not linear in the estimation parameters $\rho(h_p)$ and H_s and second, a simple least squares process will overweight residuals at the lowest altitude and nearly ignore residuals a few scale heights above the reference altitude. One approach is to use $\log(\rho)$ as the observable and write the equation as

$$\log\rho(h) = a\log\rho_p + b(h - h_p) \tag{3}$$

where a and b are the regression parameters. The equation is linear in a and b and the least squares method, within the linear regime, now minimizes the sum of squares of the density difference divided by the density, i.e. the fractional deviation in the density. This approach provides equal weight to high or low density data and is more suitable when scale height is among the estimated parameters. This model can, to a limited extent, provides asymmetric temporal variation like the left panel in Figure 4, but the inbound and outbound altitude profiles will be identical so that the model is a straight line in the left panel. Clearly equation (3) is not applicable early and late in the

AB pass when accelerometer data noise produces negative density. This model is simple and captures the dominate local variations in density. It also permits prediction of the atmospheric density at the next periapsis by assuming that the scale height is the same for the next orbit and that the density at periapsis can be obtained fromequation (1) at the next periapsis. Since the AB pass is not vertical, the two parameters in this model also absorb an unknown amount of along track variation. The persistence results in Figure 2 show the real world limitations to this approach.

Quadratic Time

In APPENDIX I it is shown that, for the constant density scale height model, the temporal variation in density in the vicinity of periapsis can be approximated by

$$\rho(t) = \rho_p \exp\left[\frac{-(t-t_p)^2}{2\sigma^2}\right] \tag{4}$$

where $$\sigma^2 = H_s r_p^2/\mu e \tag{5}$$

depends on orbit parameters and scale height. Again, to assure linear estimation, logρ is used as the observable and $a=\log\rho_p$ and $b=-1/2\sigma^2$ are the parameters. This model has the advantage that a precision trajectory is not required to generate altitude vs. time. To predict to other altitudes, the scale height can be approximated from the solution for σ^2. It is seen that a disadvantage is that the model is symmetric in time about the time of periapsis and that maximum density occurs at periapsis, whereas few of the Martian density profiles satisfy either of these conditions. A shift in the time of maximum density is easily accomplished by adding a linear term to get

$$\log\rho(t) = a\log\rho(t_p) + b(t-t_p) + c(t-t_p)^2 \tag{6}$$

which is still symmetric in time but centered at the maximum density which occurs at $t_{max}=t_p-b/2c$ and has a value of $\exp(a+b(t_{max}-t_p)/2)$. This model (QdT) does however permit different inbound and outbound altitude profiles, but with the same scale height.

Cubic and Quartic Time

One can introduce both asymmetry and a shift in the time of maximum density by extending the quadratic model to either a cubic (CubT) or a quartic model (QtT) in time, e.g.

$$\log\rho(t) = a\log\rho(t_p) + b(t-t_p) + c(t-t_p)^2 + d(t-t_p)^3 + e(t-t_p)^4 \tag{7}$$

The quartic term might be included to assure that density decreases with altitude outside the data set or to provide a better estimate of the maximum density during the pass. There are profiles for which e>0, so this model would not be recommended for extrapolation. For both models, H_s can be extracted from the quadratic coefficient. However, it was found that the $(t-t_p)^4$ term often absorbed enough of the quadratic dependence that the H_s estimates were substantially biased. Consequently, no further consideration will be given to the quartic representation.

Constant Scale Height with Time

A hybrid model (CSHT), with constant scale height but different density profiles for the inbound and outbound legs, can be obtained by adding a linear time term to equation (3) to get

$$\log\rho(h,t) = a\log\rho_p + b(h-h_p) + c(t-t_p) \tag{8}$$

where the reference altitude and time are taken at periapsis. The model permits some variation in local scale height with altitude. It is unlikely that this model should be used to extrapolate beyond the data interval, since, unless c=0, the predicted density will eventually increase with altitude.

Constant Inbound and Outbound Scale Heights

Another three parameter hybrid model is one that permits different inbound and outbound scale heights but only one density at periapsis (CSHIO).

Periapsis Timing Estimator

Satellite ephemeris propagation errors are usually dominated by along track deviations which for AB are manifested as time of periapsis errors. The PTE[14] was consequently designed to adjust the flight sequence so that it would be centered on the centroid of the density history. Based on the PTE Δt from one orbit, the initiation of the AB sequence for the next orbit is adjusted by Δt. PTE was run in shadow mode and validated during ODY and was operational for MRO. Although the details are not exactly known, results of the above models will be compared to an implementation based on Reference 14. The implementation is a simple density weighted time from periapsis to provide the location of the density centroid relative to periapsis

$$\Delta t = \sum t_i \rho_i / \sum \rho_i \tag{9}$$

where time is measured from periapsis and the sum is taken over all the density data above a threshold determined by the density noise level.

Single Orbit Examples

Each of these models was applied to the four Odyssey orbits in Figure 6. Data within 14 km altitude of periapsis are used for the LS solutions. Results are shown in Figure 8 for both density vs. time and density-altitude profiles, where the density data are shown as dots. Relevant solution parameters for these orbits are tabulated in Table 1. For the QdT and CubT models, the scale height was calculated using Equation (5) where the position and velocity at periapsis was used to calculate the eccentricity. For orbits 44, 157 and 280, little difference between the models is seen in the plots. In fact, for these orbits, the CSHT and time quadratic (QdT) models are nearly identical and the differences in the parameters in the Table 1 are ignorable. Examination of the orbit 44 profile shows that the cubic (CubT) model is beginning to diverge above 110 km and ρ=10 kg/km^3 with one branch going to zero density and the other going to an infinite density with further increase in altitude. To fit the "flat" top of orbit 157, all models prroducec a very large scale height near 23 km, whereas the remaining orbits .. have scale heights of less than 11 km. Similar statements can be made for the time of the maximum density. Estimation of the scale height is very consistent among the models, but of course all the orbit 157 estimates are much greater than

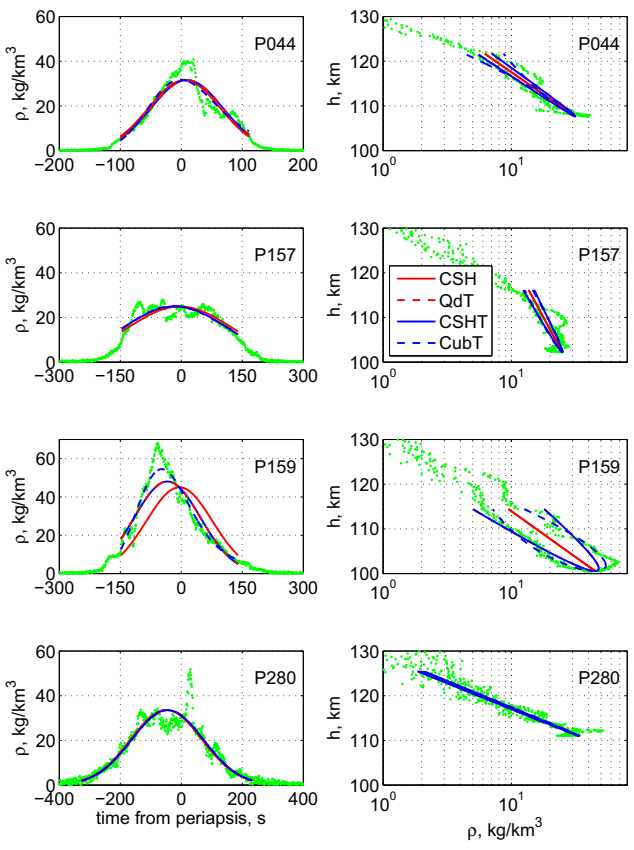

Figure 8. Density model least square fits to four Odyssey orbits. Data range δh=14 km.

estimates from nearby orbits and it would likely be unwise to use the anomalistically large scale height for orbit 157 to predict the density for orbit 158. In fact, to do so would give 21.8 kg/km^3 verses the measured value of 38.8. Predicting orbit 159 from the 157 values gives 21.9 kg/km^3. Orbits like this demonstrate the need to combine estimates from a number of orbits and even then, large differences might be expected

Table 1: Model Comparisons for Four Odyssey Orbits

Model	Odyssey Orbit			
	44	157	159	280
	ρ_{max}, kg/km^3			
Data	40.8	27.8	68.1	51.8
CSH	31.5	24.9	45.0	33.6
QdT	31.6	25.0	48.0	33.5
CSHT	31.6	25.0	48.1	33.6
CubT	31.7	25.1	54.5	33.6
	t_{max}, sec			
Data	20.0	-44.5	-58.5	29.5
CSH	5.0	-3.5	-4.5	-49.4
QdT	9.0	-15.5	-34.5	-45.4
CSHT	9.0	-15.5	-34.5	-46.4
CubT	-1.0	-19.5	-48.6	-44.4
PTE	6.8	-5.4	-28.6	-41.3
	Hs, km			
CSH	8.6	23.1	8.9	5.1
QdT	8.7	23.6	9.2	5.0
CSHT	8.6	23.1	8.9	5.1
CubT	8.3	23.8	9.7	5.0

Multiple Orbit Comparisons

The four algorithms in Table 1 and the CSHIO algorithm were applied to all three Mars missions. Only data during the "main" AB phase were included. In addition, MGS data for orbits 910 through 980 were also excluded because of an onboard computer issue that significantly reduced the quality of the accelerometer data. There is a subtle difference in how the data are selected for the three constant scale height models and the two time polynomial models. For the former, data are selected within a specified altitude range of periapsis, which for all these results is 14 km or about 2 density scale heights. Unless periapsis is at the equator or a pole, planetary flattening results in these data being asymmetric in time. Conversely, for the latter two models, the data are selected symmetric in time around periapsis with a time interval that corresponds to a planetocentric radius change of 14 km. The resulting in planetodetic altitude distribution is generally asymmetry. This small difference has a noticeable effect on the results.

Density: As a basis for comparison, the "mean" density for each orbit was calculated by averaging all five solutions for density at periapsis. Results are presented as ratios of recovered density to this mean density. For MGS it was found that this ratio varied from 0.92 to 1.06. The orbit average difference between CSH and CSHIO had a μ=0.0045 with σ=0.02 and between QdT and CubT $\mu<10^{-5}$ and $\sigma<10^{-3}$. Because these pairs of recoveries are so similar, only one of the pair

will be shown for some of the results. Figure 9 shows these ratios for the CSH, CSHT and QdT methods. There are couple of general trends evident. First, when the CSH ratios are generally greater than one, the QdT ratios are generally less than one. Second, the CSHT method provides results closest to unity over the entire mission. Third, there are two places where all three methods give nearly the same density, near orbits 860 and 1190. It will be seen in the next paragraph that a couple of these trends can be explained in terms of the method for selecting data as discussed above and the time between periapsis and the minimum planetodetic altitude. The ODY and MRO analyses showed similar trends in density ratio ranging from 0.92 to 1.06, model agreement near the pole, and CSH and QdT providing opposite deviations from unity. The CSHT model providing result closer to the mean than the other two models, but with slightly larger deviations than MGS.

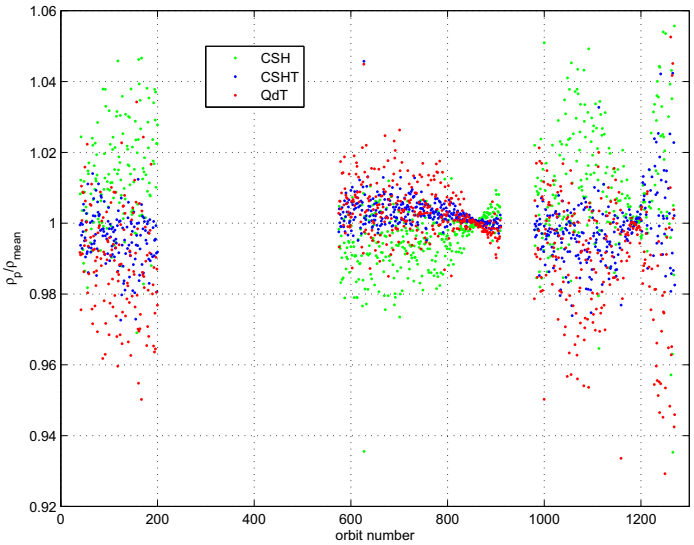

Figure 9. MGS estimated periapsis density for three methods normalized by mean periapsis density of all five methods.

Time of Maximum Density: Consider Figure 10 which shows the time from periapsis to the time when the various models predict the maximum density. For the CSH model, this is time from periapsis to minimum planetodetic latitude, i.e. the same "time to minimum altitude" presented in Figure 7. Time difference changes slowly because latitude and orbit eccentricity are changing slowly until near the final orbits when the orbit is nearly circular. During the first 200 orbits, MGS is passing from north to south as periapsis regresses northward. Consequently, minimum altitude occurs after periapsis. The CSHT and QdT results suggest there is an additional effect that further delays the time. This would be consistent with a equatorward increase in density, which is a general trend. The periapsis regresses past the equator on orbit 860 and here the altitude data distribution will be symmetric in time and conversely. So, the models should predict essentially the same atmospheric parameters. It is seen from Figure 9 that this is true for density, but not so for the δt values. Again there is an along track density gradient that delays the epoch of maximum density. At the risk of over analysis, one possibility is that the maximum density is occurring in the northern hemisphere

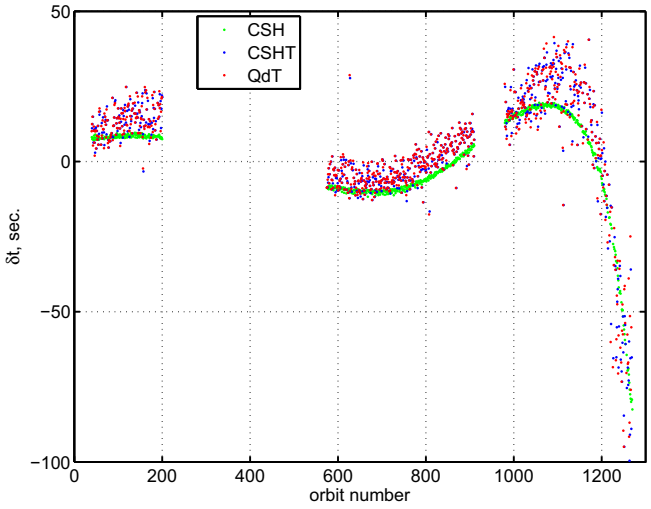

Figure 10. MGS time from periapsis to time of maximum density as predicted by three models.

since during all of phase 2, L_s (Figure 1) is between 0^o and 90^o, so it is hemisphere spring and the Sun is in the northern hemisphere. The balance of the orbits after 860 are readily explained by a minimum density occurring at the pole. Maximum positive δt occurs near orbit 1060 as periapsis regresses past 45^o latitude, the region of maximum gradient in the planetocentric altitude. As periapsis passes over the pole, there will be symmetry in the data distributions and the densities are nearly identical. One final note, the difference between the δt for CSHT and QdT has a μ=0.2 sec. and σ=1.9 sec. These two methods are providing excellent agreement in δt.

ODY and MRO analyses provided similar results. MRO had generally smaller deviations from the δt caused by flattening than MGS. ODY on the other hand, while periapsis regressed toward the pole, showed up to 40 sec. positive δt deviations which rapidly switched to negative values up to -40 sec. while moving away from the pole. Perhaps these large, rapid variations were due to the polar warming.

Density Scale Height: H_s is **t**he final variable of interest for predicting the periapsis density at subsequent orbits. As might be expected, the estimation of scale height is more sensitive than density to the altitude span of the data set. Orbit 157 in Figure 8 illustrates the difficulty. The solution used data within δh=14 km of periapsis, i.e. about two expected scale heights. The resulting H_s=23 km given in Table 1 is not a realistic value to use for predicting density at the next periapsis. From the figure it can be expected that as the altitude range δh is increased, the value of H_s would decrease perhaps to more realistic values, but the estimated periapsis density will likely increase. The data above 100 km appears to follow a straight line with a scale height of about 7.5 km, but using just these data would yield a periapsis density of about 100 kg/km^3. Hence, using a much larger data set would lead to a significantly higher prediction. Orbit 158 occurred 1 km lower in altitude than 157 and had a density of 41 kg/km^3. So the predictions using a 14 km altitude range underestimated the density for 158 and using a very large altitude range would have overestimated the density. Studies for all missions using δh=7, 11, 14 and 21 km altitude ranges showed that for orbits with "bell shaped" density histories, even with time shifts, the estimates of H_s generally differed by less than 0.5 km between the 11 and 14 km cases and 0.3 km between the 14 and 21 km cases. Differences between the 7 and 14 cases were around 1 km. For orbits that vary significantly for the "bell shape," the results are mixed. Using an altitude interval of δh=2H_s seems to be a reasonable compromise.

Like the other parameters, the estimation of H_s within a family of methods e.g. (CSH, CSHT, CSHIO) or (QdT, CubT) were very consistent with standard deviations for the differences of less than σ=50m. Between the two families σ<500m. Consequently, only the CSHT results are shown in Figure 11. The means of the three MGS data segments (6.9, 7,3, 6.6) have trends that are consistent with temperature decreasing toward the poles. The standard deviations are 1.1, 0.7 and 1.1 km, from left to right. ODY scale heights (i.e. temperature) were the means of discovering the polar warming but outside the polar region the mean scale

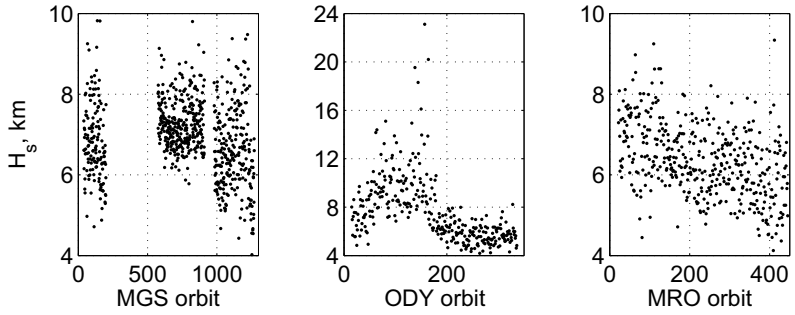

Figure 11. Density scale height recovered using the CSHT method and δh=14 km.

height drops to about 5.6 km, well below the expected value. Global circulations model simulations of a polar warming[15] show strong adiabatic heating near the pole due to subsiding flow and an adjacent region of cooling. This region is likely the reason for these small scale heights. In this region σ=0.76 km. MRO also shows a decreasing H_s trend as periapsis regresses toward the pole. If there was a sudden south polar warming, it occurred after periapsis passed the pole. Averaging over 100 orbit blocks, $H_s$varies from μ=6.9 and σ=0.86 to μ=5.7 and σ=1 km over the mission.

AEROBRAKING CORRIDOR MAINTENANCE

As mentioned earlier, a model of atmospheric density has a couple of purposes: (1) to quantify characteristics of the atmosphere for the current pass which might be used for heating calculations[18], (2) to provide a prediction of the characteristics of the next pass, and (3) provide information needed to calculate the orbit trim maneuvers to stay in the AB corridor.

Corridor Maintenance Maneuvers

To maintain the AB corridor, orbit trim maneuvers are generally performed near apoapsis to adjust the altitude of subsequent periapses and thereby control the atmospheric density.[20] For tangential, impulsive maneuvers, the first order δV_a required at apoapsis to raise periapsis altitude by an amount δr_p is first given for two body motion and the secondly is given by relating the altitude change through the CSH model to obtain the desired fractional change in periapsis density $\delta\rho_p/\rho_p$

$$\delta V_a = \frac{n}{4}\sqrt{\frac{r_a}{r_p}}\ \delta r_p = -\frac{n}{4}\sqrt{\frac{r_a}{r_p}}H_s\left(\frac{\delta\rho_p}{\rho_p}\right) \tag{10}$$

where δr_p has been approximated by δh_p, n is the orbital mean motion, r_a (r_p) is the apoapsis (periapsis) radius and H_s and ρ_p are the expected density scale height for the next orbit. Even without a precision trajectory, the previous results strongly suggest that the latter two variables are likely to contribute the majority of the uncertainty in calculating the desired δV_a.

Predicting Atmospheric Parameters for the Next Pass

For autonomous AB it will be necessary to have a prediction of atmospheric density for the next pass through the atmosphere. From past experience with Mars AB it is clear that there are likely to be large variations between predicted and observed density that are not within the current ability to predict from either empirical or numerical models of the atmosphere. Any of the density models discussed above might be used to generate parameters for predicting the conditions at the next periapsis as was demonstrated in the study of "persistence." All the models have persistence values that deviate up to a factor of 2 from unity. This naturally raised the question if some averaging of the estimates would produce a better "prediction" ratio. As mentioned, for both Magellan and MGS, some form of atmospheric density was averaged over a number of orbits to be used to predict the density at the next periapsis. Using the extensive set of data from Mars, a study was performed of two averaging methods over a range of altitudes (δh) used to obtain model coefficients and over the number of orbits used in the averaging process. One would anticipate both of these variables would influence the results. Only the CSH and CSHT models were included as CSH is the simplest model and CSHT provided prediction results that were the closest to the average of all the methods. The data collection altitude ranges studied were δh=7, 10, 14 and 21 km. This range starts near the mean H_s averaged all latitudes and times. The values of 10 and 14 can be thought of as 1.5 or 2 times the H_s=7 km value or 1 and 1.5 times the H_s~10 that was seen during the polar warming. The number of orbits for the averaging was varied from 1 to 20. It might be anticipated that a low number of averaging orbits will have a large standard deviation for the

prediction ratio while estimates using very long data arcs may be biased by the time dependent (latitudinal, seasonal, diurnal) variations in atmospheric characteristics.

Figure 12 show the results for MGS. The prediction σ is the standard deviation over all the values of the ratio of observed to predicted density across the entire mission. Two simple averaging methods were explored for both the CSH and CSHT models. For notational convince, let n+1 be the orbit number at which density is to be estimated using model values from orbits n, n-1,...n-k+1, where k is the "number of orbits in the estimate." When the number of orbits in the estimate k=1, the prediction value is the standard deviation of all the points in Figure 9 for each model. For the "CSH AVG" results the previous k values of 'a' and 'b' in equation (3) are used to get a value of 'a' at the periapsis altitude of orbit n+1. These k values are simply averaged to obtain the "estimated" density at orbit n+1. This value is used in the denominator of the prediction ratio. A similar process is used for the CSHT model where the time dependence in this model is ignored. The second averaging method attempted to account for the "accuracy" of the estimated parameters. The LS process was turned into a WLS method by using the reciprocal of the rms deviation between observed and model predicted density to "weight" the data. Orbits with large deviations, like orbit 159 (Figure 8), would be weighted lower than orbits which had a smaller rms, like orbit 280. So the second method is the weighted sum of the estimates, much like a minimum variance linear combination of random variables. No probabilistic interpretation is attempted for these results for obvious reasons.

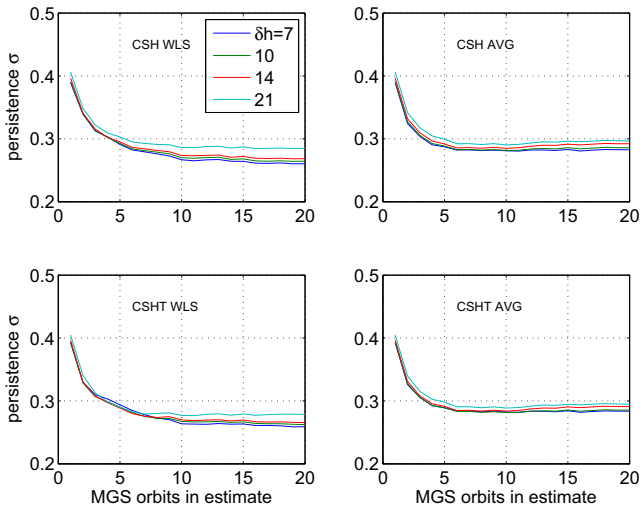

Figure 12. .Density prediction capability of various methods for the MGS mission

Referring to the figure, the standard deviation across all orbits starts near 40% 1σ. The initial downward trend as the number of orbits increases is to be expected. From a practical standpoint little is to be gained in reducing σ after 10 to 15 orbits and the AVG results start to increase slightly after 10 orbits are averaged. The three lower values of δh provide similar results and noticeable lower than the δh=21 case, although this different is likely not significant from an autonomous AB standpoint. This residual deviation of about 28% is interpreted as the natural variability of the atmosphere and can not be reduced without significantly more knowledge of the atmosphere than is available from onboard measurements alone. The standard deviation does not tell the whole story on prediction for autonomous AB. The probability of the ratio being greater than a specified value may be more relevant. The gamma distributions shown in Figure 3 provide a more rigorous means of making probabilistic statements. Here a simpler approach is taken by just tracking the fraction of total orbits for which the ratio of observed to predicted density ratio exceeds 1.5. For MGS this result is shown in Figure 13 for the same methods and data as Figure 12. There appears to be little advantage to using more than 10 to 15 orbits for the prediction and WLS provides about 1% improvement over the AVG approach. Note that

WLS is computationally more cumbersome than the AVG approach, which is a consideration for onboard computation. For prediction the shorter data spans, δh<10 provided a small advantage, for Figure 13 the lines cross repeatedly with δh=14 being lower than the others in more cases. Setting δh at about 2 scale heights may be a good rule of thumb and unless time of maximum density is a desirable parameter to estimate, the simple CSH method seems like a good candidate. Selecting between AVG and WLS is less obvious.

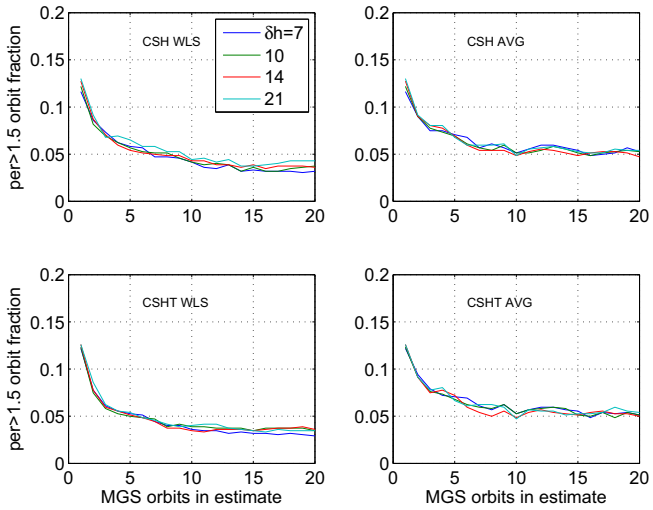

Figure 13. Fraction of the total MGS orbits for which the ratio of observed density to predicted density exceeded 1.5.

Just to complete this story, similar results are shown for ODY and MRO in Figure 14 for just the CSH model and the WLS prediction method. The ODY prediction has a minimum at 0.3 which is 10% higher than either MGS or MRO, but still over a 30% reduction below the initial persistence values. This higher variability also appears in the prediction greater than 1.5 have nearly 10% of the orbits above this limit. Also the longer the span of orbits used in the prediction, the smaller the σ. The δh=21 appears to be optimal for ODY, consistent with ODY having Hs>10 km for a significant fraction of the mission. Of course, MRO behaves in a different manner from the other two missions with an initial rise in σ followed by a steep fall eventually arrived 0.28 like MGS. The decline in the 1.5 fraction is slower than MGS, but does get near 5% eventually.

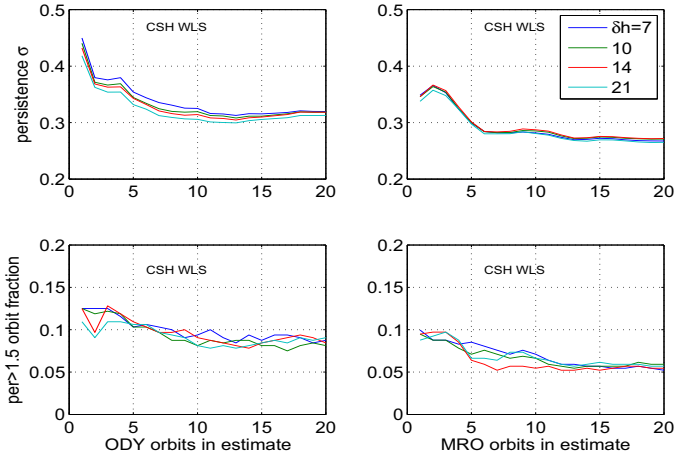

Figure 14. prediction and orbit fractions for ODY and MRO.

SUMMARY

1. Mars is a challenging environment for autonomous aerobraking due to the large, natural orbit to orbit variability in the density profiles. With the plethora of data from MGS, ODY and MRO, some latitudinal seasonal trends have been identified, but, the best that can be done to date is to reduce the variability by about one third.

2. Because of thermospheric waves due to thermal tides in the lower atmosphere, aerobraking in temporate latitudes has nearly twice the average variability as aerobraking near the poles.

3. Five different formulations for the density variation with altitude and time were investigated. If maximum density or the time of maximum density are not relevant, then the simple constant density scale height model (CSH) performs nearly as well as more complicated models. If time is important, the hybrid CSHT is the likely choice.

4. Two methods were used to combine data from numerous orbits to improve the prediction for subsequent orbits. A weighted least squares method performed a little better than simple averaging, but at the cost of additional software on the vehicle. Both methods reduced the variability by about 30%. The remaining 1σ deviations of about 30% are likely due to natural variability that will have to be included in vehicle design.

5. Similar analyses can not be performed for aerobraking at Venus and Titan due to lack of data. However, significant orbit to orbit variation has been noted at Venus and gravity waves have been seen at both bodies. Because of the basic physics, neither body will likely be as challenging as Mars, but prudence suggest not attempting autonomous aerobraking until more is known about the atmospheres.

ACKNOWLEDGEMENT

This work was sponsored by the NASA Engineering and Safety Center (www.nesc.nasa.gov). This assessment can be found in the final report NESC-RP-09-00605 in November 2011.

REFERENCES

1. Willcockson, W. H., Magellan Aerobraking Control Corridor: Design and Implementation, *Adv. Astronautical Sciences*, Vol. 87, Part II, 1994, pp. 647-662.
2. Spencer, D. A. & Tolson, R. H., "Aerobraking Cost and Risk," *J. Spacecraft and Rockets,* Vol. 44, No. 6, Nov.-Dec., 2007, pp.1285-1293
3. Tolson, R. H., Keating, G. M., Zurek, R. W., Bougher, S. W., Justus, C. J., Fritts, D. C., "Application of Accelerometer Data to Atmospheric Modeling During Mars Aerobraking Operations." *J. Spacecraft and Rockets*, Vol. 44, No. 6, 2007, pp. 1171-1179.
4. Konopliv, A. S. & Sjogren, W. L., "Venus Gravity Handbook," JPL Pub.96-2, Jan. 1996.
5. Striepe, S. A., Blanchard, R. C., Kirsch, M. F., Fowler, W. T.,"Huygens Titan Probe Trajectory Reconstruction Using Traditional Methods and the Program to Optimize Trajectories II", AAS/AIAA Space Flight Mechanics Meeting, Sedona, AZ, 2007, AAS 07-226.
6. Muller-Wodarg, I. C. F., Yelle, R. V., Borggren, N., Waite, J. H., "Waves and horizontal structures in Titan's thermosphere," *J. Geophysical Research,* Vol. 111, A12315, doi:10.1029/2006JA011061, 2006.
7. Keating, G. M., et al.,"Models of Venus Neutral Upper Atmosphere: Structure and Composition," *Adv. Space Res.*, Vol, 5, No. 11, 1985, pp. 117-171.
8. Lyons, D. T., Beerer, J. G., Esposito, P., Johnston, M. D., "MGS: Aerobraking Mission Overview," *J. of Spacecraft and Rockets,* Vol. 36, No. 3, 1999, pp. 307-313.
9. Tolson, R. H., Keating, G. M., Cancro, G. J., Parker, J. S., Noll, S. N., and Wilkerson, B. L., "Application of Accelerometer Data to Mars Global Surveyor Aerobraking Operations," *J. Spacecraft and Rockets*, Vol. 36, No. 3, May-June, 1999, pp. 323-329.
10. Hanna, J. L. & Tolson, R. H., "Approaches to Autonomous Aerobraking at Mars," AAS/AIAA Astrodynamics Specialist Conference, Quebec City, Canada, July 30-August 2, 2001. AAS 01-387
11. Justus, C. G., Duvall, A., Keller, V. W., "Atmospheric Models for Aeroentry and Aeroassist," Proceedings of the 2nd International Planetary Probe Workshop, NASA Ames

Research Center, Moffett Field, CA, pp 41-48, August 23-27, 2004. Also published in NASA/CP-2004-213456, April 2005.

12. Keating, G.M., et al., "Detection of winter polar warming in Mars upper atmosphere," Paper PS1.02-1TH2A-006, EGS XXVII General Assembly, Nice, France, April 2002.
13. Dec, J. A., Gasbarre, J. F., George, B. E., "Thermal Analysis and Correlation of the Mars Odyssey Spacecraft's Solar Array During Aerobraking Operations," AIAA/AAS Astrodynamics Conference, Monterey CA, Aug. 5-8, 2002.
14. Willcockson, W. H. & Johnson, M. A., "Mars Odyssey Aerobraking: The First Step Towards Autonomous Aerobraking Operations" 2003 IEEE Aerospace Conference, Big Sky, MT, March 9-14, 2003.
15. Bougher, S. J., Bell, J. M., Murphy, J. R., Lopez-Valverde, M. A., Withers, P. G., "Polar warming in the Mars thermosphere: Seasonal variations owing to change in insolation and dust distributions," *Geophysical Research Letters*, Vol. 33, 2006.
16. Wilson, R. J., "Evidence for nonmigrating thermal tides in the Mars upper atmosphere from the MGS Accelerometer Exp.", *Geophys. Res. Lett.*, 27(21), 3563-3566, 2002.
17. Dwyer, A. M., Tolson, R. H., Munk, M. M., Tartabini, P. V., "Development of a Monte Carlo Mars-GRAM Model for Mars 2001 Aerobraking Simulations," J. of the Astronautical Sciences, 2001, Vol. 109, pp 1293-1308.
18. Dec, this conference
19. Fritts, D. C., Wang, L., Tolson, R. H., "Mean and gravity wave structured and variability in the Mars upper atmosphere inferred from Mars Global Surveyor and Mars Odyssey aerobraking densities," *J. Geophy. Res.,* Vol. 111, 2006.
20. Maddock, this conference
21. King-Hele, D. G., "Satellite Orbits in an Atmosphere: Theory and Applications," Blackie and Sons, Ltd., Glasgow and London, 1987, ISBN 0-216-92252-6.

APPENDIX I

Aerobraking in a Constant Density Scale Height Atmosphere

Consider an AB pass for which atmospheric density can be modelled using equation (1). To produce the familiar "bell" shaped density vs. time profile,[21] assume two body motion about a spherical planet and expand the altitude in a Taylor series about the time of periapsis to get

$$h(t) = h(t_p) + \frac{1}{2}\ddot{h}(t_p)(t - t_p)^2 + O((t - t_p)^4) \qquad \text{(A-1)}$$

where $\ddot{h}(t_p)$ is the second derivative of altitude with respect to time evaluated at periapsis. Under the above assumptions, altitude is symmetric in time so odd derivatives vanish and the truncated terms are of order $(t\text{-}t_p)^4$ and negligible for most AB orbits. Eliminating altitude in equation (1) in favor of time in equation (A-1) yields the "bell" shape variation of density with time,

$$\rho(t) = \rho(t_p)\exp\left[\frac{-\ddot{h}(t_p)(t-t_p)^2}{2H_s}\right] \tag{A-2}$$

The $\ddot{h}$ term can be written in terms of the orbit parameters as $\ddot{h}(t_p) = \mu e / r_p^2$, giving a function of scale height, orbit eccentricity, periapsis distance and gravitational constant (μ). To demonstrate the "square root of scale height" law, start with the Gaussian density function

$$f(x,\xi,\sigma) = \frac{1}{\sigma\sqrt{2\pi}}\exp\left[-\frac{(x-\xi)^2}{2\sigma^2}\right] \tag{A-3}$$

where ξ is the mean and σ is the standard deviation and $\int_{-\infty}^{\infty} f(x)dx = 1$.

The last two equations suggest the substitution $\sigma^2 = H_s/\ddot{h}_p = H_s r_p^{\,2}/(\mu e)$, leading to

$$\rho(t) = \rho(t_p)\sqrt{\frac{2\pi r_p^2 H_s}{\mu e}}\left[\frac{1}{\sigma\sqrt{2\pi}}\exp\left[\frac{-(t-t_p)^2}{2\sigma^2}\right]\right] = \rho_p\exp\left[\frac{-(t-t_p)^2}{2\sigma^2}\right] \tag{A-4}$$

and the integral over the entire pass is

$$\int_{-\infty}^{\infty}\rho(t)dt = \rho(t_p)\sqrt{\frac{2\pi r_p^2 H_s}{\mu e}} \tag{A-5}$$

This result shows that the integral of ρ is proportional to the density at periapsis times the square root of H_s. Since the velocity decrease due to drag is approximately proportional to the integral of ρ, over estimation of the scale height will result in underestimating the density as determined by an OD approach that process tracking data before and after the unobserved AB pass.

The only approximation to arrive at (A-4) and (A-5) is the truncation of the Taylor series and as long as the scale height is small compared to the periapsis altitude, the higher order terms are not significant. For example, for Mars with e=0.1, H_s=7 km, h_p=125 km, and $\rho_p = 50\,\text{kg/km}^3$, the error in altitude is less than 1 km and the error is density is less than 0.1 kg/km^3 over an altitude range from periapsis to 5 scale heights above periapsis.

The integrals of dynamic pressure ($\frac{1}{2}\rho V^2$) for total drag effect or heat flux ($\frac{1}{2}\rho V^3$) for total heat input may be more important variables than density. Under the same assumptions for which (A-5) is valid, the velocity variation throughout the AB pass varies by only a few percent from the value at periapsis. So the total heat input during a pass is closely approximated by the value of the heat flux at periapsis times the radical in (A-5).

Finally, the "drag duration" (T_d) is often defined as the time from the inbound occurrence of 1% of maximum density to the outbound time when the density is 1% of maximum density, then the drag duration is twice the time for the spacecraft to increase in altitude above periapsis by $4.6H_s$. From A-2 and A-5

$$T_d = 2\sqrt{\frac{9.2H_s r_p^2}{\mu e}} \qquad \text{(A-6)}$$